

# Assessment of seasonal groundwater quality and potential saltwater intrusion: a study case in Urmia coastal aquifer (NW Iran) using the groundwater quality index (GQI) and hydrochemical facies evolution diagram (HFE-D)

Vahab Amiri<sup>1</sup> · Mohammad Nakhaei<sup>1</sup> · Razyeh Lak<sup>2</sup> · Majid Kholghi<sup>3</sup>

Published online: 14 June 2015  
© Springer-Verlag Berlin Heidelberg 2015

**Abstract** Coastal aquifers are at threat of salinization in most parts of the world. This work investigated the seasonal hydrochemical evolution of coastal groundwater resources in Urmia plain, NW Iran. Two recently proposed methods have been used to comparison, recognize and understand the temporal and spatial evolution of saltwater intrusion in a coastal alluvial aquifer. The study takes into account that saltwater intrusion is a dynamic process, and that seasonal variations in the balance of the aquifer cause changes in groundwater chemistry. Pattern diagrams, which constitute the outcome of several hydrochemical processes, have traditionally been used to characterize vulnerability to sea/saltwater intrusion. However, the formats of such diagrams do not facilitate the geospatial analysis of groundwater quality, thus limiting the ability of spatio-temporal mapping and monitoring. This deficiency calls for methodologies which can translate information from some diagrams such Piper diagram into a format that can be mapped spatially.

Distribution of groundwater chemistry types in Urmia plain based on modified Piper diagram using  $GQI_{Piper(mix)}$  and  $GQI_{Piper(dom)}$  indices that Mixed Ca–Mg–Cl and Ca–HCO<sub>3</sub> are the dominant water types in the wet and dry seasons, respectively. In this study, a groundwater quality index specific to seawater intrusion ( $GQI_{SWI}$ ) was used to check its efficiency for the groundwater samples affected by Urmia hypersaline Lake, Iran. Analysis of the main processes, by means of the Hydrochemical Facies Evolution Diagram (HFE-Diagram), provides essential knowledge about the main hydrochemical processes. Subsequently, analysis of the spatial distribution of hydrochemical facies using heatmaps helps to identify the general state of the aquifer with respect to saltwater intrusion during different sampling periods. The HFE-D results appear to be very successful for differentiating variations through time in the salinization processes caused by saltwater intrusion into the aquifer, distinguishing the phase of saltwater intrusion from the phase of recovery, and their respective evolutions. Both GQI and HFE-D methods show that hydrochemical variations can be read in terms of the pattern of saltwater intrusion and groundwater quality status. But generally, in this case (i.e. saltwater and not seawater intrusion) the HFE-D method was presented better efficiency than GQI method (including  $GQI_{Piper}$  and  $GQI_{SWI}$ ).

✉ Vahab Amiri  
vahab.amiri@gmail.com

Mohammad Nakhaei  
nakhaeimohammad@yahoo.com

Razyeh Lak  
lak\_ir@yahoo.com

Majid Kholghi  
kholghi@ut.ac.ir

**Keywords** Groundwater · Saltwater intrusion · GQI · HFE-D · Urmia Lake

- <sup>1</sup> Department of Applied Geology, Faculty of Earth Sciences, Kharazmi University, Tehran, Iran
- <sup>2</sup> Research Institute for Earth Sciences, Geological Survey of Iran, Tehran, Iran
- <sup>3</sup> Department of Irrigation and Reclamation Engineering, Faculty of Agriculture and Natural Resources, University of Tehran, Tehran, Iran

## 1 Introduction

Contamination of freshwater resources caused by saltwater intrusion is a critical issue, which can effect on water quality, vegetation, soil conditions and even ecosystem

along coastal lines. Salt/seawater intrusion can cause adverse and long-term impacts on coastal groundwater systems and limit their use as a supply of good quality water for domestic, agricultural and industrial purposes (Perera et al. 2009). Proximity to seawater and some anthropogenic activities (such as over-exploitation) associated with coastal areas result in degradation of freshwater resources in coastal aquifers. Saline/saltwater intrusion is caused mainly by the decrease of groundwater table or by increasing the seawater levels. When groundwater is pumped from a coastal aquifer, the freshwater level is lowered and the sea intrudes into the aquifer (Qahman et al. 2005). Therefore, the amount of freshwater stored in the aquifer is decreased.

The chemical composition of groundwater in coastal aquifers is typically controlled by mixing of fresh and saline water of various origins and also by water–rock interaction processes such as cation exchange, redox reactions, carbonate mineral dissolution and precipitation as well as evaporation, salt-precipitation processes and migration and seepage of saltwater (Vengosh 2003; Appelo and Postma 2005; Capaccioni et al. 2005; De Montety et al. 2008; Lucas et al. 2010; Panteleit et al. 2011; Zghibi et al. 2013; Chen and Jiao 2014; Boluda-Botella et al. 2014). The sources of freshwater in coastal aquifers is typically limited to precipitation, river water or irrigation water whereas the source of salt in groundwater (independent of the original source of the water itself) can be of meteoric origin, from water–rock interaction, salts derived from remnant formation water trapped in sediments and anthropogenic salts that may include salts from irrigation, salt/seawater bodies, wastewater, road salt and gypsum applied to improve agricultural soil quality (Marie and Vengosh 2001; Vengosh 2003; Qahman et al. 2005; Misut and Voss 2007; El Yaouti et al. 2009; Mollema et al. 2013; Bouzourra et al. 2014).

To preserve coastal groundwater, the sources of saline water and mechanisms of mobility require to be recognized for sustainable development of groundwater resources (Gibbs et al. 2013). There are different methods to assessment of water quality in the coastal areas. Some of the common methods used to study the water quality of aquifers include hydrogeochemical methods (Ravikumar and Somashekar 2011; Al-Taani 2012; Mustapha et al. 2012), geophysical investigations (Kashouty et al. 2012), multivariate techniques (Huang et al. 2011), and remote sensing with GIS (Pradhan 2009; Pradhan and Pirasteh 2011; Ketata et al. 2012). Among all these, geochemical method is one of the widely used.

The present study has been carried out within the Urmia plain, next to the Urmia Lake. This Lake, one of the largest hypersaline lakes of the world, is located in northwest of Iran. It is a natural asset with considerable ecological,

environmental, and cultural values (Bakhtiari et al. 2011; Abbaspour et al. 2012). Urmia Lake is registered under Ramsar Convention as a habitat of international significance for birds and some rare species. The Lake is a National Park and has been recognized by UNESCO as a Biosphere Reserve. In 1985, the Lake had a surface area of about 5000 km<sup>2</sup>, mean depth of 6 m, and an elevation of 1275.6 m above the mean sea level. The approximate length and width of the Lake were 140 and 40 km, respectively (Marjani and Jamali 2014). This hypersaline lake lies in the center of a closed drainage basin (with almost 52,000 sq.km), with all surface and groundwater draining towards Urmia Lake. The particular geology of the basin and the high evaporative and continuous deposition of salts lead to hypersaline conditions. The Lake is surrounded by a number of important freshwater-brackish satellite wetlands, several of which are also of global significance for their biodiversity. For the last decade, Urmia Lake has been in a critical condition, as a result of declining water levels and increasing salinity (Ministry of Energy 2010). There is considerable evidence that groundwater resources are already being exploited at rates faster than aquifer recharge in the Urmia Lake watershed area (Wada et al. 2010; Hassanzadeh et al. 2011). Surface water flows are being diverted for use at rates which do not allow adequate inflow to Urmia Lake to maintain the lake's current level (Eimanifar and Mohebbi 2007; Hoseinpour et al. 2010; Reveshty and Maruyama 2010; Hassanzadeh et al. 2011). Water use within the Urmia Lake basin at current rates is unsustainable without loss of the lake, and the consequent environmental damage as well as damage to the surrounding groundwater resources, population and agriculture.

The hydrogeology and hydrochemistry of the whole coastal area of Urmia plain has not been systematically studied yet, although the extent of soil and groundwater pollution in some areas surroundings of Urmia Lake has been surveyed in recent years. This study is an attempt to show the relationship between hydrochemical variations and the pattern of potential saltwater intrusion. For this purpose, this study uses concepts from the recently published development of a groundwater quality index for seawater intrusion in coastal aquifers (Tomaszkiewicz et al. 2014), which derived by combining the seawater fraction index ( $GQI_{f_{sea}}$ ) and the freshwater-seawater mixing index ( $GQI_{Piper(mix)}$ ) of the Piper diagram and Hydrochemical Facies Evolution Diagram (HFE-D, Giménez-Forcada 2010). As mentioned before, the objective of present study is to compare three methods (i.e.  $GQI_{Piper}$ ,  $GQI_{SWI}$  and HFE-D) to assess what effects saltwater intrusion may have on groundwater quality. All computations carried out in the Microsoft Excel environment. In addition, some results are quantified and translated to map format using a Geographical Information System (GIS).

## 2 Materials and methods

### 2.1 Theoretical background

#### 2.1.1 Piper diagram

The Piper diagram can be divided into six differing domains: I, II, III, IV, V, VI, representing Ca-HCO<sub>3</sub>, Na-Cl, Mixed Ca-Na-HCO<sub>3</sub>, Mixed Ca-Mg-Cl, Ca-Cl, and Na-HCO<sub>3</sub> type waters, respectively (Fig. 1) (Subramani et al. 2005; Sarath Prasanth et al. 2012). In this diagram, saltwater locate in domain II and freshwater is generally represented in domain I. Mixing of seawater and freshwater is defined by a horizontal line through the center of the diagram (GQI<sub>Piper(mix)</sub>) which can range from 0 for hypersaline water to 100, representing highly freshwater and computed numerically by Eq. 1:

$$GQI_{Piper(mix)} = \left[ \frac{Ca^{2+} + Mg^{2+}}{\sum Cations} + \frac{(HCO_3^-)}{\sum Anions} \right] \times 50(\text{in meq/l}) \quad (1)$$

For more details and investigation of the other domains (Fig. 1), GQI<sub>Piper(mix)</sub> can be used with another index, GQI<sub>Piper(dom)</sub> (Eq. 2) simultaneously, which ranges from 0 to 100 for Ca-Cl type waters (domain V) and Na-HCO<sub>3</sub> type waters (domain VI), respectively (Tomaszkiewicz et al. 2014):

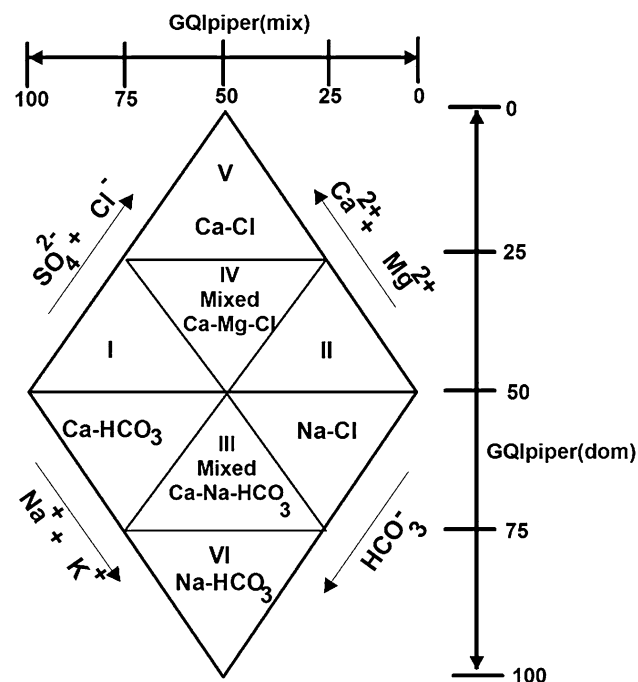


**Fig. 1** Definition of piper domains based on GQI<sub>Piper(mix)</sub> and GQI<sub>Piper(dom)</sub> indexes (developed by Tomasziewicz et al. 2014)

$$GQI_{Piper(dom)} = \left[ \frac{(Na^+ + K^+)}{\sum Cations} + \frac{(HCO_3^-)}{\sum Anions} \right] \times 50(\text{in meq/l}) \quad (2)$$

#### 2.1.2 Saltwater fraction as a groundwater quality index

In order to determine the extent of saline water intrusion, a theoretical mixture percentage (Eq. 3) was proposed considering Cl<sup>-</sup> as a conservative ion (Appelo and Postma 2005). In this equation, all Cl<sup>-</sup> is assumed to originate from saltwater sources (e.g. a lake). So, by considering this fact that the current investigation carried out in an aquifer adjacent a saltwater source, the saline water contribution (f<sub>lake</sub>) in a groundwater sample considered to have formed from a mixture of saline water and freshwater has been calculated from its Cl<sup>-</sup> content as follows:

$$f_{lake} = \frac{C_{Cl,sample} - C_{Cl,fresh}}{C_{Cl,lake} - C_{Cl,fresh}} \times 100 \quad (3)$$

where C<sub>Cl, sample</sub> is the Cl<sup>-</sup> concentration of the groundwater sample, C<sub>Cl,lake</sub> is the Cl<sup>-</sup> concentration of the lake and C<sub>Cl,fresh</sub> indicates the Cl<sup>-</sup> concentration of the local freshwater. Saltwater fraction (f<sub>lake</sub>) ranges from 0 to 100 and one can investigate an index GQI<sub>flake</sub> (Eq. 4):

$$GQI_{flake} = (1 - f_{lake}) \times 100 \quad (4)$$

#### 2.1.3 Saltwater intrusion groundwater quality index (GQI<sub>SWI</sub>)

Tomaszkiewicz et al. (2014) concluded that saltwater fraction has weaknesses and if one apply it alone (i.e. without other indexes), it maybe not be useful. So they proposed a combinative index which designated as GQI<sub>SWI</sub> (Eq. 5) and is derived equally from values of GQI<sub>Piper(mix)</sub> (Eq. 1) and GQI<sub>flake</sub> (Eq. 4):

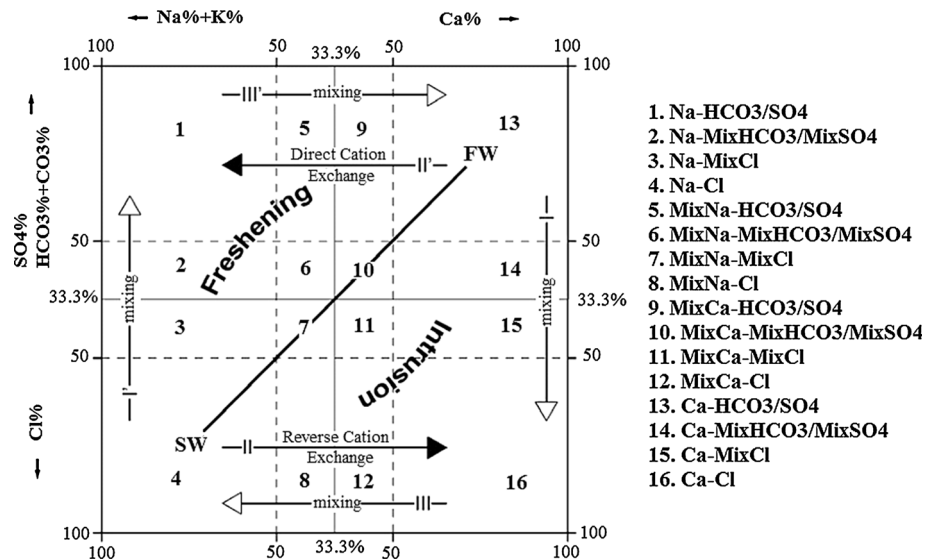
$$GQI_{SWI} = \frac{GQI_{Piper(mix)} + GQI_{flake}}{2} \quad (5)$$

It should be note that in the current study we are used the hydrochemical properties of a hypersaline lake to calculations; therefore instead for sea, all formulas are presented for lake.

#### 2.1.4 Hydrochemical facies evolution of groundwater in the saline water intrusion process

The Hydrochemical Facies Evolution Diagram (HFE-D) which proposed by Gimenez Forcada (2010) provides an easy way to identify the state of a coastal aquifer with respect to intrusion/freshening phases that takes place over time and which are identified by the distribution of anion

**Fig. 2** HFE diagram (Giménez-Forcada 2010)



and cation percentages in the square diagram (Fig. 2). The HFE-D considers just the percentage of the major cations ( $\text{Ca}^{2+}$  and  $\text{Na}^+$ ) and anions ( $\text{HCO}_3^-$ ,  $\text{SO}_4^{2-}$  and  $\text{Cl}^-$ ) which determine the dynamics of saline/saltwater intrusion. When complex processes are simplified it is inevitable that certain lower order considerations are sacrificed. This occurs when the discussion does not take into account the ions occupying a secondary position in the two end members (freshwater and saline/saltwater), as is the case for  $\text{SO}_4^{2-}$ ,  $\text{Mg}^{2+}$ , and  $\text{K}^+$  (Ghiglieri et al. 2012). The sulfate percentage is considered an alternative to bicarbonate percentage because both can represent the major anion in the freshwater. The  $\text{Mg}^{2+}$  ion has an irregular behavior in exchange reactions and for this reason  $\% \text{Mg}^{2+}$  is not taken into account in the exchange processes. Lastly, the percentage sodium incorporates the percentage of potassium, as the concentration of  $\text{K}^+$  is generally much lower than that of  $\text{Na}^+$ .

In the intrusion stage, the aquifer is affected by two almost simultaneous processes, namely an increase in salinity (line I), which triggers reverse exchange reactions (line II). The result is the characteristic Ca-Cl facies. Thereafter, the groundwater composition evolves (line III) towards saline/saltwater (Na-Cl). During the freshening process, freshwater recharge induces direct exchange reactions (lines I' and II'), resulting in the formation of a Na-HCO<sub>3</sub> facies. Finally, the water evolves along line III' towards the composition of the freshwater which enables the recovery of the aquifer (Giménez-Forcada 2010).

## 2.2 Study area

Urmia Plain is in the northwest of Iran. This region is located between the eastern longitude of 44°, 20' and 45°, 20' and northern latitude of 37°, 05' and 38°, 05' (Fig. 3).

Groundwater resources in Urmia Plain are very important sources of water. The underground aquifer of this plain is a large natural collecting reservoir and regulator of water inflowing from the large drainage area, which both retains water and enables its useful utilization. The groundwater flow direction is from west to east (Urmia Lake). Hydrological investigations have shown that this underground reservoir spreads under an area of approximately 868 km<sup>2</sup> and consists of confined and unconfined aquifers (Badv and Deriszadeh 2005). Nazlu-Chai, Rowzeh-Chai, Shahr-Chai and Baranduz-Chai are the four main rivers, which are flowing in the plain. They originate from the western mountainous area and end in Urmia Lake.

This area is in a Mediterranean pluvial seasonal-continental climate according to the Global Bioclimatic Classification System. During recent 30-year period mean annual temperature and precipitation in the area are 11.52 °C and 346.3 mm, respectively, while mean maximum temperature occurs in July (31.2 °C) and minimum in January (-6.1 °C) (NOAA 2012; WMO 2014).

## 2.3 Water sampling and analyses

In this study, 141 groundwater samples were collected during June 2014 (wet season) and September 2014 (dry season) from shallow and deep wells and hand dug wells (depths: 10–120 m) distributed throughout the coastal area (see Figs. 5 and 7) using standard sampling procedures (APHA 1985; ISO 5667-11:1993). Water samples were collected from pumping wells after minimum of several hours of pumping prior to sampling in order to remove any standing water from the wells. At each sampling point, samples were stored in two 250 ml polyethylene bottles after being filtered through 0.45 μm membrane filters and



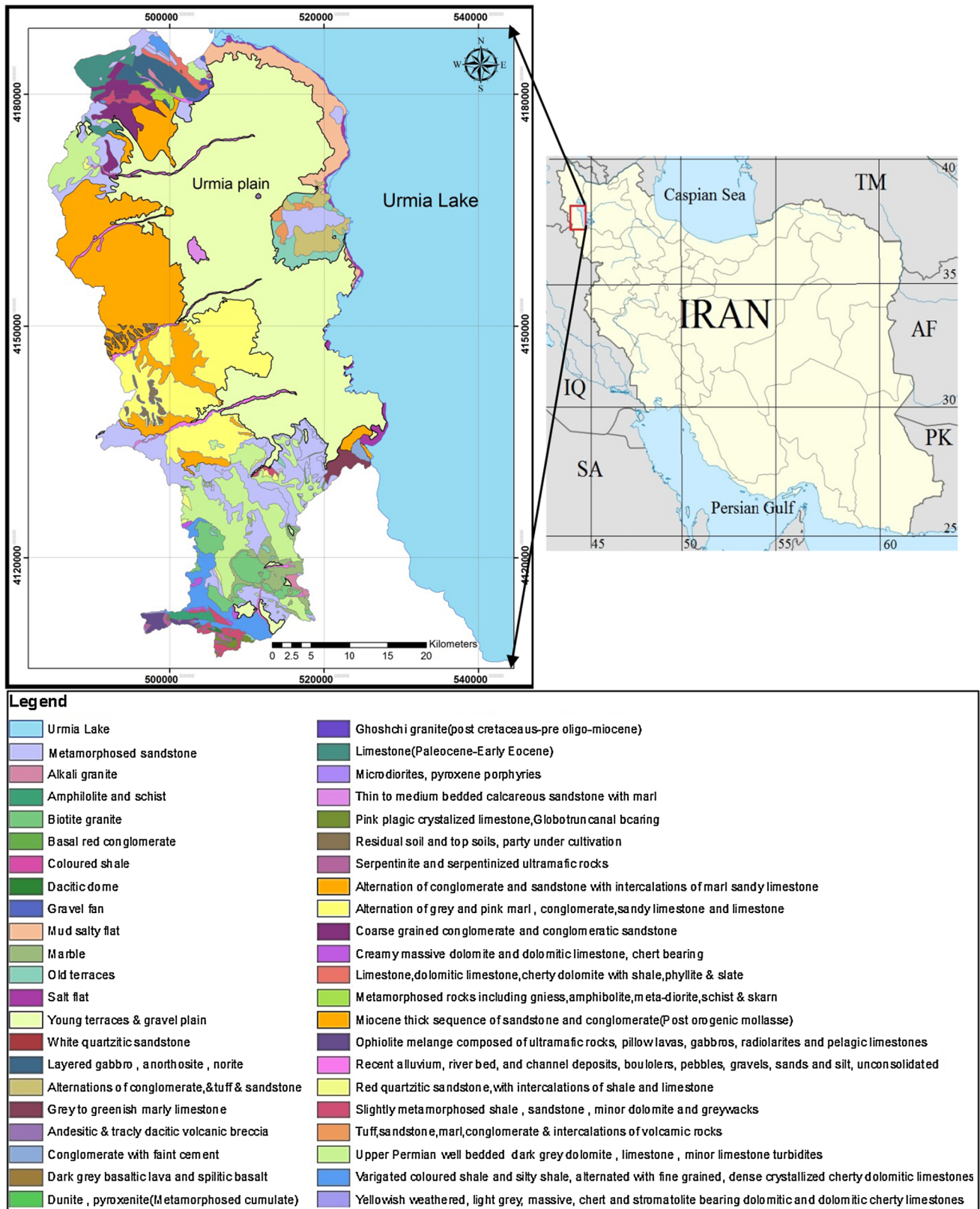


Fig. 3 Geological map of the study area

**Table 1** Results of groundwater quality analysis for study area

Parameter	Wet season						Dry season					
	Groundwater			Urmia Lake water			Groundwater			Urmia Lake water		
	Min	Max	Mean	Min	Max	Mean	Min	Max	Mean	Min	Max	Mean
pH	6.87	8.42	7.24	6.35	6.41	6.38	6.98	8.92	8.3	6.55	6.6	6.57
Eh	−62.87	26.08	4.84	n.m.	n.m.	n.m.	−88	0.6	−75.8	n.m.	n.m.	n.m.
DO	0.58	4.5	1.16	n.m.	n.m.	n.m.	0.07	3.6	1.85	n.m.	n.m.	n.m.
T	14	20	16.67	22	22.7	22.7	13.5	23	20	23	24	23.5
EC	355	3800	1171.89	127,900	133,950	130,800	428	7180	1505.4	187,380	192,500	189,940
Ca <sup>2+</sup>	3.54	319.9	105.11	113.2	130.7	121.27	6.11	271.5	105.6	57.4	57.9	57.65
Mg <sup>2+</sup>	5.67	485.8	78.48	62,500	65,550	64343.64	15.6	345	79	40,420	40,518	40,469
Na <sup>+</sup>	15.5	1080.7	130.38	51,000	58,770	54827.27	12.2	1229	177.89	9850	9877	9863.5
K <sup>+</sup>	0.78	114.63	10.39	12,730	13,800	13279.09	2.6	118.8	10.44	17,920	17,987	17953.5
HCO <sub>3</sub> <sup>−</sup>	15.9	10132.1	402.95	7191.8	9205.5	7984.18	30.2	734.4	306.51	13664.3	13685.4	13674.85
CO <sub>3</sub> <sup>2−</sup>	24.7	605.5	103.34	7073.9	9054.5	7853.27	93.5	625.3	213.85	21504.5	21,675	21589.75
Cl <sup>−</sup>	6.1	1325	116.23	160443.6	175811.8	166870.3	7.4	2061.4	200.69	252687.2	253585.1	253136.2
SO <sub>4</sub> <sup>2−</sup>	1	980	153.95	2900	3200	3036.36	1	590	143.63	56,000	56,700	56,350

Dissolved oxygen (DO); cations and anions are in mg/L; temperature (T) is in °C; Electrical Conductivity (EC) is in  $\mu\text{S}/\text{cm}$ ; Redox potential (Eh) is in mV; Min: Minimum; Max: Maximum; n.m.: not measured

were divided into two groups: (1) filtered non-acidified for anion analysis, and (2) filtered acidified (with a few drops of Suprapur<sup>®</sup> nitric acid (HNO<sub>3</sub>, 65 % v/v; Merck, Germany)) for cation and major elements analysis. At each sampling point, pH and electrical conductivity (EC) parameters were measured in the field condition using a HACH Multimeter device (HACH, Germany). The collected samples were kept in an ice box and then transferred to a fridge where they were stored at 4 °C until delivery to the Zarazma Mineral Studies Company (ZMSC), Iran, for analyses. The outcomes of the both surveys are presented in Table 1.

### 3 Results and discussion

Piper diagram has been designed by calculation of  $GQI_{\text{Piper(mix)}}$  and  $GQI_{\text{Piper(dom)}}$  indexes for samples collected in wet and dry seasons. Results show that in wet period, samples N27, S04, S30 and S36 (i.e. 4.6 %) locate in field II (saline water). Samples S39 and N21 are in domain III and VI, respectively (type waters Mixed Ca–Na–HCO<sub>3</sub> and Na–HCO<sub>3</sub>). Most of samples have type water Mixed Ca–Mg–Cl (domain IV) and Ca–Cl (domain V), and 20 samples (i.e. 23.8 %) are freshwater (domain I), (Fig. 4a). In dry period, number of samples with saltwater composition (domain II) has been increased to 8 samples; include N1, N17, N27, N34, S30, S36, S39 and ST39 (i.e.

14 %) and in contrast with wet period, predominate type water (i.e. 56.4 %) is fresh (domain I). In general 22.8 % samples locate in mixed domain (III and IV) and the rest are situated in domains V and VI (about 7 %) (Fig. 4a).

Distribution of groundwater chemistry types in Urmia plain based on modified Piper diagram using  $GQI_{\text{Piper(mix)}}$  and  $GQI_{\text{Piper(dom)}}$  indices in both wet and dry seasons is presented in Fig. 5. As shown, there are three main water types in the wet season including Mixed Ca–Mg–Cl, Ca–Cl and freshwater. In the wet season, the near shore samples in the both northern and southern parts of Urmia plain show that the dominant water type is Mixed Ca–Mg–Cl. In this case, the Urmia hypersaline lake may be considered as the main source of Cl<sup>−</sup> and conclude that the intrusion of saltwater is occurred but the dominant water types in the dry season clearly demonstrate that the groundwater exploitation for some uses such as agriculture leads to movement of groundwater from recharge zones (western mountains) and finally freshening the water samples. Therefore, in spite of some near shore sampling points with the Na–Cl water type (red circles in Fig. 5), it can be concluded that there is no much interaction between Urmia aquifer and Urmia Lake.

The  $GQI_{\text{SWI}}$  can range between 0 and 100, where 0 is indicative of saltwater and 100 represents freshwater. In general, index values are above 75 for freshwater and below 50 for saline groundwater and saltwater based on comparison with the literature. Mixed groundwater has a  $GQI_{\text{SWI}}$  between 50 and 75. The corresponding  $GQI_{\text{SWI}}$

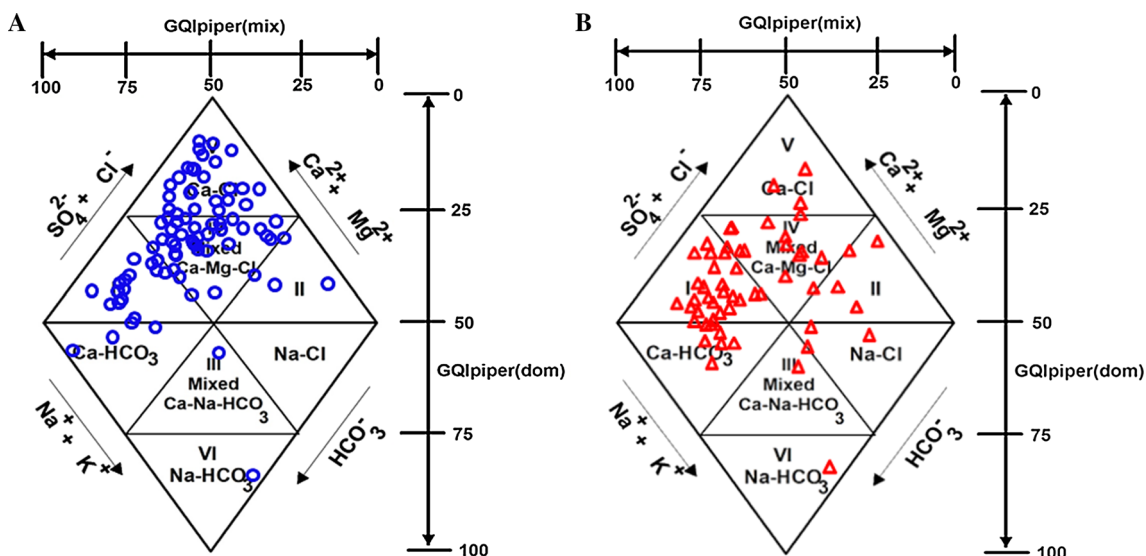


**Fig. 4** Representation of groundwaters sampled in **a** June 2014 and **b** September 2014 in the Piper diagram

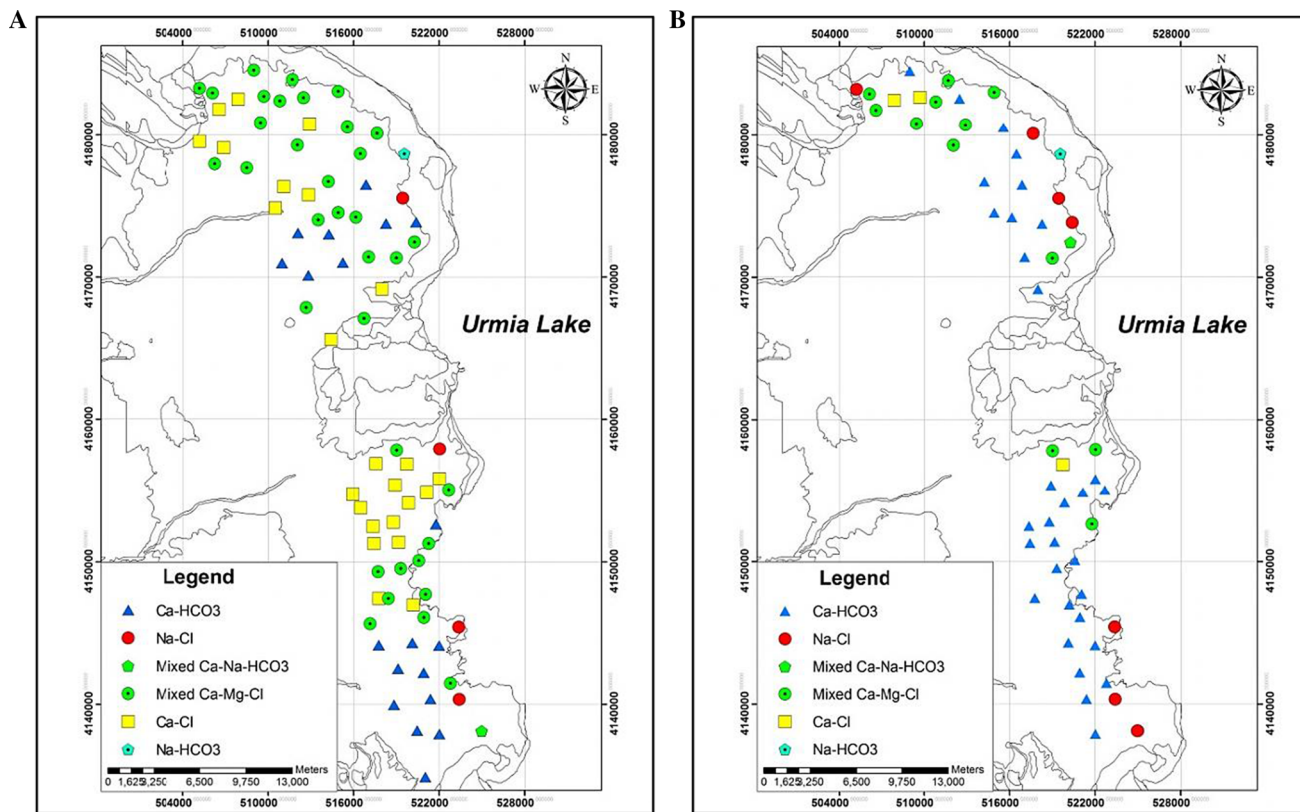


**Fig. 5** Distribution of water chemistry types in Urmia plain based on modified Piper diagram using  $GQI_{Piper(mix)}$  and  $GQI_{Piper(dom)}$  indices in **a** wet and **b** dry seasons

confirms that there are none samples in the range of salt-water (Table 2) and in compare with piper, 63.1 and 64.91 % of samples have freshwater compositions, respectively. It seems that piper diagram can show quality

of groundwater better than the proposed  $GQI_{SWI}$  index by Tomaszekiewicz et al. (2014) which is based on considering the  $Cl^-$  concentration of seawater (calculation of saltwater fraction). The  $Cl^-$  concentration of hypersaline lake is

**Table 2** Results of  $GQI_{SWI}$  calculations for water samples in wet and dry seasons

Water type	Typical $GQI_{SWI}$		$GQI_{SWI}$ for Urmia groundwater samples							
	Min	Max	Wet season (June 2014)				Dry season (September 2014)			
			Min	Max	Mean	No. of samples (%)	Min	Max	Mean	No. of samples (%)
Freshwater	75	100	75.11	94.54	81.58	53 (63.10)	75.33	91.09	84.24	37 (64.91)
Mixed groundwater	50	75	54.08	74.93	67.80	27 (32.4)	51.01	72.75	65.79	18 (31.58)
Saline groundwater	10	50	24.46	48.40	37.98	4 (4.76)	25.01	46.89	35.95	2 (3.51)
Saltwater	0	10	–	–	–	–	–	–	–	–

more times of the  $Cl^-$  concentration of seawater and groundwater samples must have a substantial  $Cl^-$  concentration to show the saline water intrusion.

Generally, use of conventional diagrams such as Piper diagram does not allow for a detailed recognition of the facies evolution sequence during recharge and intrusion events. Giménez-Forcada (2010) has suggested that the HFE-D diagram is more informative for this purpose. The HFE diagram for Urmia groundwater samples in both wet and dry seasons are presented in Fig. 6. The freshwaters belong to the  $Ca-HCO_3/SO_4$  (13) and saline waters show the  $Na-Cl$  (4) facies. Results show that in both wet and dry seasons, most of the water samples followed the succession of facies along the mixing line (4-7-10-13) which demonstrates simple mixing with little or no intervention of base-exchange reactions. During the phase of Urmia water intrusion, to the right and beneath horizontal line 33.3 %, there is an initial increase in salinity and a rapid reverse exchange of  $Na^+/Ca^{2+}$ , which is recognized by the characteristic  $Ca-Cl$  facies (16) (evolution 13-14-15-16). In Urmia plain, existence of two samples (N11, S3) in parts 15, 16 (wet season) and sample S2 in part 15 (dry season) show the facies influenced by inverse cationic ( $Na^+/Ca^{2+}$ ) exchange reactions. This type of water evolves toward facies that are closer to sea water ( $Na-Cl$ ) (4) (evolution 16-12-8-4). In the freshening stage, to the left and above the horizontal line 33.3 %, direct exchange processes occur more slowly; the water gain  $Na^+$  and cede  $Ca^{2+}$  until  $Na-HCO_3/SO_4$  (1) facies is achieved (evolution 4-3-2-1). In Urmia groundwater resources, locating some samples (black points) in parts 1, 2, 5, 6 in wet and 1, 2 in dry seasons indicate the overlapping in mixing line between fresh and saltwater caused by direct cation exchange process. In Urmia Plain, the facieses  $Na-HCO_3/SO_4$  (1),  $Na-MixHCO_3/MixSO_4$  (2),  $MixNa-HCO_3/SO_4$  (5) and  $MixNa-MixHCO_3/MixSO_4$  (6) are reached in wet season. In dry season, only the facieses  $Na-HCO_3/SO_4$  (1) and  $Na-MixHCO_3/MixSO_4$  (2) are reached.

In Table 3, the hydrochemical facieses of Urmia groundwater samples based on the HFE diagram in wet and dry seasons are presented. Results indicate that more than

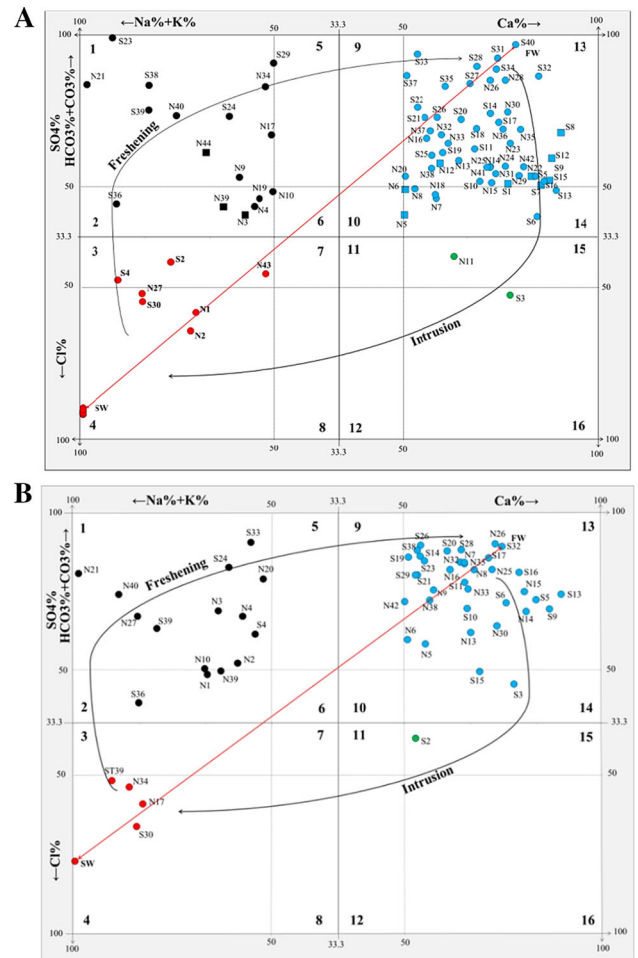


**Fig. 6** HFE diagram for Urmia groundwater samples in **a** wet and **b** dry seasons (N#, S#: samples collected in the northern and southern parts of the Urmia plain; square symbol:  $SO_4^{2-}$  water in freshening stage; ST39 and S39 are sampled at the same location, ST39 from the upper unconfined aquifer and S39 from confined aquifer)

52 and 57 % of samples collected from northern part of Urmia aquifer have  $Ca-HCO_3/SO_4$  facies for wet and dry seasons, respectively. Also, 70 and 65 % of groundwater samples of southern part show the  $Ca-HCO_3/SO_4$  facies for wet and dry seasons, respectively.



**Table 3** Hydrochemical facies of groundwater samples based on HFE diagram

Period	Sample location	HFE facies	No. of sample	Percent
Wet season	Northern part (N samples)	Na-HCO <sub>3</sub> /SO <sub>4</sub>	6	13.64
		Na-MixHCO <sub>3</sub> /MixSO <sub>4</sub>	5	11.36
		Na-MixCl	1	2.27
		Na-Cl	3	6.82
		Ca-HCO <sub>3</sub> /SO <sub>4</sub>	23	52.27
		Ca-MixHCO <sub>3</sub> /MixSO <sub>4</sub>	5	11.36
		Ca-MixCl	1	2.27
	Total		44	100
	Southern part (S samples)	Na-HCO <sub>3</sub> /SO <sub>4</sub>	5	12.50
		Na-MixHCO <sub>3</sub> /MixSO <sub>4</sub>	1	2.50
		Na-MixCl	2	5
		Na-Cl	1	2.50
		Ca-HCO <sub>3</sub> /SO <sub>4</sub>	28	70
		Ca-MixHCO <sub>3</sub> /MixSO <sub>4</sub>	2	5
Ca-Cl		1	2.50	
Total		40	100	
Dry season	Northern part (N samples)	Na-HCO <sub>3</sub> /SO <sub>4</sub>	8	28.58
		Na-MixHCO <sub>3</sub> /MixSO <sub>4</sub>	2	7.14
		Na-Cl	2	7.14
		Ca-HCO <sub>3</sub> /SO <sub>4</sub>	16	57.14
	Total		28	100
	Southern part (S samples)	Na-HCO <sub>3</sub> /SO <sub>4</sub>	4	13.79
		Na-MixHCO <sub>3</sub> /MixSO <sub>4</sub>	1	3.45
		Na-Cl	2	6.90
		Ca-HCO <sub>3</sub> /SO <sub>4</sub>	19	65.52
		Ca-MixHCO <sub>3</sub> /MixSO <sub>4</sub>	2	6.90
	Ca-MixCl	1	3.45	
Total		29	100	

The aquifer vulnerability maps to saltwater intrusion were prepared based on calculations of  $GQI_{SWI}$  and HFE diagrams for both wet and dry seasons. Based on  $GQI_{SWI}$  method, the vulnerability maps (Figs. 7a, b) for Urmia Lake saltwater intrusion confirms that the study area has generally freshwater in both wet season (mean  $GQI_{SWI} = 81.58$ ) and dry season (mean  $GQI_{SWI} = 82.8$ ). However, some signs of saltwater intrusion are evident, in both wet and dry seasons, along the coastline due to proximity to the Urmia hypersaline Lake. In addition, indications of saltwater intrusion can be discerned in the northern half of the study area, near the Nazlu-Chai River as saltwater may be conveyed in the riverbed during dry season in particular due to minimal discharge.

Distribution of groundwater types for wet and dry seasons indicate that water quality classification based on HFE diagram (Figs. 7c, d) is more precise than  $GQI_{SWI}$  based classification. In general, when groundwater exploitation is significantly reduced, the direction of coastal flow in the aquifer system reverses from landward to lake/seaward.

The aquifer will resume the natural condition: the aquifer receives recharge from infiltration through the shallow soil and through the outcrops of the aquifer near the mountain. The aquifer system will be controlled mainly by topography-driven flow, and this will lead to gradual freshening of the coastal aquifer that had ever experienced saltwater intrusion. As showed in Figs. 7c, d, some sampling points which are close to the coast have the sub-stage 1, 2, 3 and 4 (indicating the dominant freshening sub-stages). This suggests that, in wet season, recharge of groundwater is important and positioning the coastal water samples in the freshening phase can prove it. In dry season, by increasing the water exploitation from the aquifer, additional saltwater intrusion is not found. The main reason may be existence the fine grain sediments in the coastal areas which acts as a natural barrier. Under this conditions, increasing the groundwater exploitation leads to movement of freshwaters from recharge zones in the western mountains not saltwater from Urmia Lake. In some areas, particularly in the southern part, there is no sign of seasonal variation in



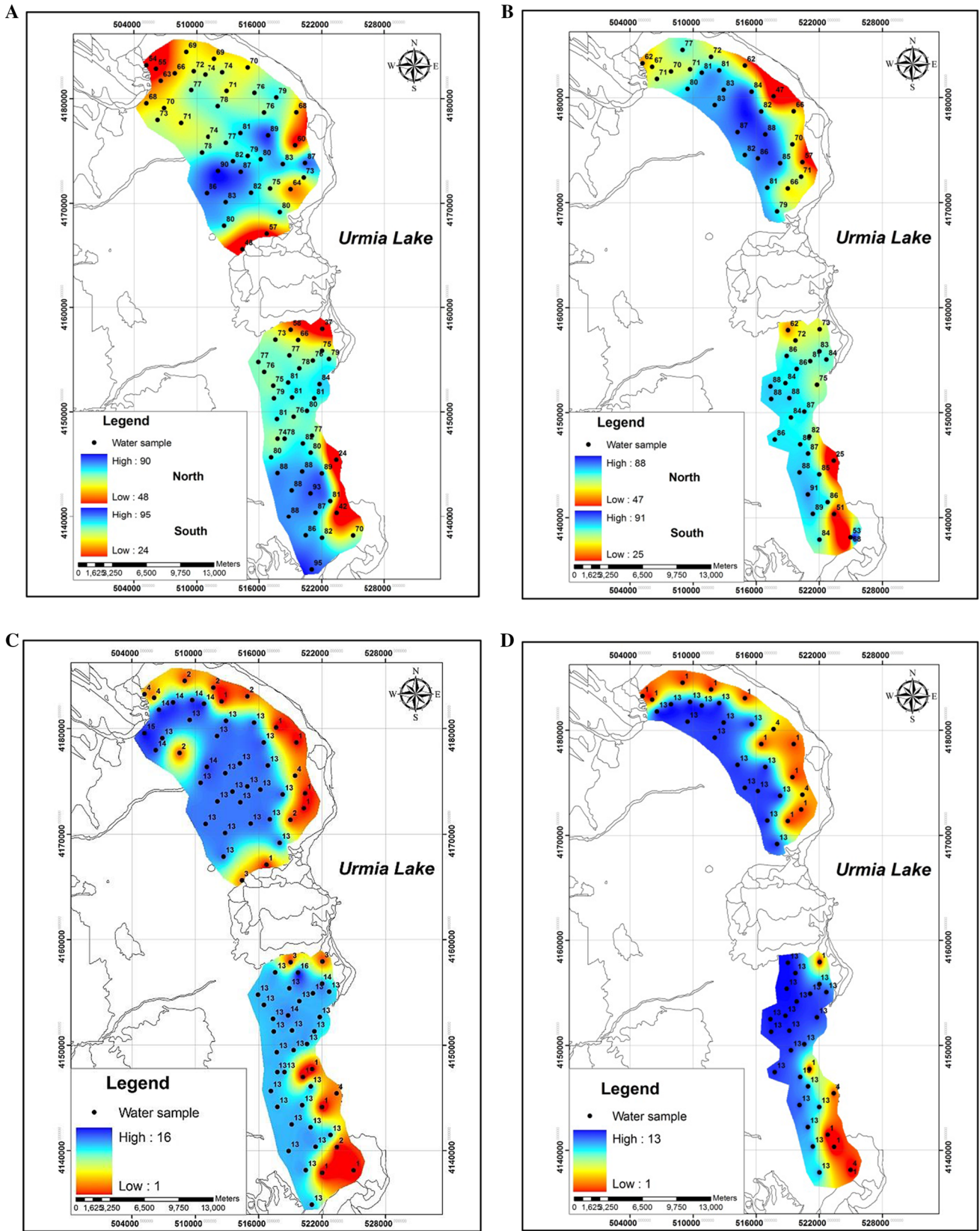


**Fig. 7** The aquifer vulnerability maps to saltwater intrusion for **a** wet and **b** dry seasons based on GQI<sub>SWI</sub> and **c** wet and **d** dry seasons based on HFE diagram. Reds indicate more saline and blues indicate more fresh samples

groundwater quality. In these areas, the groundwater overflow to the lake can be concluded.

#### 4 Conclusion

This study investigated the seasonal hydrochemical evolution of coastal groundwater resources in Urmia plain, based on two recently proposed methods to recognize and understand the temporal and spatial evolution of saltwater intrusion in a coastal alluvial aquifer. At first, we used Piper diagram by calculation of  $GQI_{\text{Piper(mix)}}$  and  $GQI_{\text{Piper(dom)}}$  indexes for samples and then compared piper's results with the other methods. Results show that in wet period most of samples have type water Mixed Ca–Mg–Cl (domain IV) and Ca–Cl (domain V) and in dry period, predominate type water (i.e. 56.4 %) is fresh (domain I). While Piper diagram can fairly separate type water but the formats of such diagrams do not facilitate the geospatial analysis of groundwater quality. This deficiency calls for methodologies which can translate information from some diagrams such Piper diagram into a format that can be mapped spatially. Results of  $GQI_{\text{SWI}}$  index show that the index is not applicable for hypersaline water conditions. Because  $GQI_{\text{SWI}}$  index uses  $\text{Cl}^-$  concentration as an important parameter in calculation of seawater fraction and in present study, concentration of  $\text{Cl}^-$  is far too more than seawater. Evaluation of water samples in the HFE diagram indicates that most groundwater samples collected from the same well during different periods in the study area still fell into the same type, which can indicate that the seasonal variability did not affect the groundwater much. Distribution of groundwater types for wet and dry seasons indicate that water quality classification based on HFE diagram is more precise than  $GQI_{\text{SWI}}$  based classification. As showed, some sampling points which are close to the coast have the sub-stage 1, 2, 3 and 4 (indicating the dominant freshening sub-stages). This suggests that, in wet season, recharge of groundwater is important and situating the coastal water samples in the freshening phase can prove it. Both GQI and HFE-D methods show that hydrochemical variations can be read in terms of the pattern of saltwater intrusion and groundwater quality status. But generally, in this case (i.e. saltwater and not seawater intrusion) the HFE-D method was presented better efficiency than GQI method (including  $GQI_{\text{Piper}}$  and  $GQI_{\text{SWI}}$ ).

**Acknowledgments** The authors would like to thank the corresponding people in the Geological Survey of Iran (GSI) for the financial support which helped to carry out this research work.

**Compliance with Ethical Standards** This study was funded by the Geological Survey of Iran (GSI). The authors declare that they have no conflict of interest. For this type of study formal consent is not required. This article does not contain any studies with human participants or animals performed by any of the authors.

#### References

- Abbaspour M, Javid AH, Mirbagheri SA, Ahmadi Givi F, Moghimi P (2012) Investigation of lake drying attributed to climate change. *Intern J Environ Sci Technol* 9:257–266
- Al-Taani AA (2012) Seasonal variations in water quality of Al-Wehda Dam north of Jordan and water suitability for irrigation in summer. *Arab J Geosci*. doi:10.1007/s12517-011-0428-y
- APHA (American Public Health Association) (1985) Standard methods of the examination of water/wastewater, 16th ed. APHA, AWWA, and WPCF, New York
- Appelo CAJ, Postma D (2005) *Geochemistry*. CRC Press, Groundwater and Pollution
- Badv K, Deriszadeh M (2005) Wellhead protection area delineation using the analytic element method. *Water Air Soil Pollut* 161:39–54
- Bakhtiari A, Zeinoddini M, Tofighi MA (2011) Effects of inflow reduction on water level, morphology and salinity pattern of the Urmia Lake. *J Hydraul* 6(3):83–93 (in Persian)
- Boluda-Botella N, Valdes-Abellan J, Pedraza R (2014) Applying reactive models to column experiments to assess the hydrogeochemistry of seawater intrusion: optimising ACUAINTRUSION and selecting cation exchange coefficients with PHREEQC. *J Hydrol* 510:59–69
- Bouzourra H, Ra Bouhlila, Elango L, Slama F, Ouslati N (2014) Characterization of mechanisms and processes of groundwater salinization in irrigated coastal area using statistics, GIS, and hydrogeochemical investigations. *Environ Sci Pollut Res*. doi:10.1007/s11356-014-3428-0
- Capaccioni B, Didero M, Paletta C, Didero L (2005) Saline intrusion and refreshing in a multilayer coastal aquifer in the Catania Plain (Sicily, Southern Italy): dynamics of degradation processes according to the hydrochemical characteristics of groundwaters. *J Hydrol* 307:1–16
- Chen K, Jiao JJ (2014) Modeling freshening time and hydrochemical evolution of groundwater in coastal aquifers of Shenzhen, China. *Environ Earth Sci* 71:2409–2418
- De Montety V, Radakovitch O, Vallet-coulomb C, Bernard Blavoux B, Hermitte D, Valle SV (2008) Origin of groundwater salinity and hydrogeochemical processes in a confined coastal aquifer: case of the Rhône delta (Southern France). *Appl Geochem* 23:2337–2349
- Eimanifar A, Mohebbi F (2007) Urmia Lake (Northwest Iran): a brief review. *Saline Syst* 3:5. doi:10.1186/1746-1448-3-5
- El Yaouti F, El Mandour A, Khattach D, Benavente J, Kaufmann O (2009) Salinization processes in the unconfined aquifer of Bou-Areg (NE Morocco): a geostatistical, geochemical, and tomographic study. *Appl Geochem* 24:16–31
- Ghiglieri G, Carletti A, Pittalis D (2012) Analysis of salinization processes in the coastal carbonate aquifer of Porto Torres (NW Sardinia, Italy). *J Hydrol* 432–433:43–51
- Gibbs MS, Dandy GC, Maier HR (2013) Assessment of the ability to meet environmental water requirements in the Upper South East of South Australia. *Stoch Environ Res Risk Assess*. doi:10.1007/s00477-013-0735-9
- Giménez-Forcada E (2010) Dynamic of seawater interface using hydrochemical facies evolution diagram. *Ground Water* 48(2):212–216
- Hassanzadeh E, Zarghami M, Hassanzadeh Y (2011) Determining the main factors in declining the Urmia Lake level by using system dynamics modeling. *Water Resour Manag* 26(1):129–145
- Hoseinpour M, Fakheri Fard A, Naghili R (2010) Death of Urmia Lake, a silent disaster investigating causes, results and solutions of Urmia Lake drying. Paper presented at the 1st international applied geological congress, Department of Geology, Islamic Azad University, Islamic Azad University-Mashad Branch, Iran

- Huang J, Ho M, Du P (2011) Assessment of temporal and spatial variation of coastal water quality and source identification along Macau peninsula. *Stoch Environ Res Risk Assess* 25(3):353–361
- ISO (International Standards Organisation) (1993) Water quality-sampling -part 11: Guidance on sampling of ground waters. ISO 5667-11
- Kashouty ME, Aziz AA, Soliman M, Mesbah H (2012) Hydrogeophysical investigation of groundwater potential in the El Bawiti, Northern Bahariya Oasis, Western Desert, Egypt. *Arab J Geosci* 5:953–970
- Ketata M, Gueddari M, Bouhlila R (2012) Use of geographical information system and water quality index to assess groundwater quality in El Khairat deep aquifer (Enfidha, Central East Tunisia). *Arab J Geosci* 5:1379–1390
- Lucas Y, Schmitt AD, Chabaux F, Clément A, Fritz B, Elsass Ph, Durand S (2010) Geochemical tracing and hydrogeochemical modelling of water-rock interactions during salinization of alluvial groundwater (Upper Rhine Valley, France). *Appl Geochem* 25:1644–1663
- Marie A, Vengosh A (2001) Sources of salinity in groundwater from Jericho area, Jordan valley. *Ground Water* 39:240–248
- Marjani A, Jamali M (2014) Role of exchange flow in salt water balance of Urmia Lake. *Dyn Atmos Ocean* 65:1–16
- Ministry of Energy (2010) Integrated management plan for Lake Urmia Basin. Internal report
- Misut PE, Voss CI (2007) Freshwater-saltwater transition zone movement during aquifer storage and recovery cycles in Brooklyn and Queens, New York City, USA. *J Hydrol* 337:87–103
- Mollema PN, Antonellini M, Dinelli E, Gabbianelli G, Greggio N, Stuyfzand PJ (2013) Hydrochemical and physical processes influencing salinization and freshening in Mediterranean low-lying coastal environments. *Appl Geochem* 34:207–221
- Mustapha A, Aris AZ, Juahir H, Ramli MF (2012) Surface water quality contamination source apportionment and physicochemical characterization at the upper section of the Jakara Basin, Nigeria. *Arab J Geosci*. doi:10.1007/s12517-012-0731-2
- NOAA (National Oceanic and Atmospheric Administration). “Oroonmeh climate normals 1961–1990”. Retrieved 27 Dec 2012
- Panteleit B, Hamer K, Kringel R, Kessels W, Schulz HD (2011) Geochemical processes in the saltwater-freshwater transition zone: comparing results of a sand tank experiment with field data. *Environ Earth Sci* 62:77–91
- Perera EDP, Jinno K, Tsutsumi A, Hiroshiro Y (2009) Numerical study of salinity variation in a coastal aquifer: a case study of the Motooka region in western Japan. *Stoch Environ Res Risk Assess* 23:957–965
- Pradhan B (2009) Ground water potential zonation for basaltic watersheds using satellite remote sensing data and GIS techniques. *Central Eur J Geosci* 1:120–129
- Pradhan B, Pirasteh S (2011) Hydro-chemical analysis of the groundwater of the Basaltic catchments: upper Bhatsai Region, Maharashtra. *Open Hydrol J* 5:51–57
- Qahman K, Larabi A, Ouazar D, Naji A, Alexander H, Cheng D (2005) Optimal and sustainable extraction of groundwater in coastal aquifers. *Stoch Environ Res Risk Assess* 19:99–110
- Ravikumar P, Somashekar RK (2011) A geochemical assessment of coastal groundwater quality in the Varahi river basin, Udipi District, Karnataka State, India. *Arab J Geosci*. doi:10.1007/s12517-011-0470-9
- Reveshty M, Maruyama Y (2010) Study of Uremia Lake level fluctuations and predict probable changes using multi-temporal satellite images and ground truth data period (1976–2010). Paper presented at the Map Asia 2010 and ISG 2010, Kuala Lumpur, Malaysia
- Sarath Prasanth S, Magesh N, Jitheshlal K, Chandrasekar N, Gangadhar K (2012) Evaluation of groundwater quality and its suitability for drinking and agricultural use in the coastal stretch of alappuzha district, kerala, india. *Appl Water Sci* 2(3):165–175
- Subramani T, Elango L, Damodarasamy S (2005) Groundwater quality and its suitability for drinking and agricultural use in Chithar River Basin, Tamil Nadu, India. *Environ Geol* 47(8):1099–1110
- Tomaszkiewicz M, Abou Najm M, El-Fadel M (2014) Development of a groundwater quality index for seawater intrusion in coastal aquifers. *Environ Model Softw* 57:13–26
- Vengosh A (2003) Salinization and saline environments. In: Sherwood Lollar, B. (Ed.), *Environmental geochemistry. Treatise on geochemistry* 9 (Holland, H.D., Turekian, K.K., Exec. Eds.), Elsevier, pp 333–365
- Wada Y, van Beek L, van Kempen C, Reckman J, Vasak S, Bierkens M (2010) Global depletion of groundwater resources. *Geophysical research letters* 37(20) <http://dx.doi.org/10.1029/2010gl044571>
- WMO (World Meteorological Organisation) (2014) <http://worldweather.wmo.int/en/city.html?cityId=1454>
- Zghibi A, Merzougui A, Zouhri L, Tarhouni J (2013) Interaction between groundwater and seawater in the coastal aquifer of Cap-Bon in the semi-arid systems (north-east of Tunisia). *Carbonates Evaporites*. doi:10.1007/s13146-013-0181-2